Table 2 Hydrolytic activity of the immobilized Chit42 on the referred substrates[a]

			Hydrolytic activity of Chit42 (%)			
Substrate	MW (kDa)	DD (%)	Free	MNPs-GA	CMS-GA	CMS-Gpn
Colloidal chitin	n.d.	≤8	100.0 ± 2.9	100.0 ± 4.2	100.0 ± 2.4	100.0 ± 8.2
QS1	98	81	14.8 ± 3.5	46.5 ± 6.1	69.0 ± 1.6	44.9 ± 4.0
QS2	31	77	13.5 ± 0.8	50.8 ± 8.0	60.7 ± 5.3	49.2 ± 7.5
CHIT100	100–300	>90	9.8 ± 3.5	34.2 ± 1.9	43.8 ± 1.4	34.5 ± 7.2
CHIT600	600–800	>90	4.2 ± 3.6	3.1 ± 2.8	14.6 ± 1.9	16.3 ± 4.5
CHIT50	50–190	77	16.0 ± 0.8	72.2 ± 4.2	98.0 ± 3.0	43.5 ± 8.6

[a] 100% activity: 5.3 U mg^{-1} of the protein, 5.6, 6.5, 6.4 U mg^{-1} of the immobilized enzyme for MNPs-GA-Chit42, CMS-GA-Chit42 and CMS-Gpn-Chit42, respectively. Data are means of three independent experiments and standard errors are indicated.

converts weak Schiff bases into stable secondary amino bonds[32] was attempted and evaluated (Fig. 3). The reduction of the immobilized catalyst caused a clear decrease of the initial Chit42 hydrolytic activity, of about 50% (from 1.0 to 0.52 units), 70% (from 1.5 to 0.42 U) and 33% (from 1.3 to 0.86 U) in the catalysts MNPs-GA-Chit42, CMS-GA-Chit42 and CMS-Gpn-Chit42, respectively. However, the reduction clearly improved the reusability of the immobilized Chit42, the MNPs-GA-Chit42 catalyst being the most favoured and retaining more than 50% of its activity after at least 5 cycles of reuse (Fig. 3). This makes the linkers stabilization an important aspect for the operational activity of the biocatalyst. Regardless of the support used, Chit42 hydrolyzed colloidal chitin and all the chitosan of different size and DD tested (Table 2). Both free and immobilized chitinase showed maximum hydrolytic activity on colloidal chitin and with more activity on small chitosan with DD 77–81 than in larger ones with DD > 90. In addition, immobilized enzyme had at least 3 times higher hydrolytic activity than free enzyme on any of the chitosan tested. Curiously, Chit42 immobilized on CMS-GA hydrolyzed commercial chitosan CHIT50 and colloidal chitin with the same effectiveness. The application of immobilized Chit42 on the production of COS was evaluated using HPAEC-PAD chromatography and mass spectrometry analyses. Independently of the type of support used, and as happened previously by using free Chit42,[8] chitobiose ($(GlcNAc)_2$) was the main product obtained from colloidal chitin, followed by $(GlcNAc)_3$ and GlcNAc when using the immobilized enzyme (Fig. 4A). In addition, a large number of masses corresponding to different series of fully acetylated and partially acetylated COS (faCOS and paCOS, respectively) were detected using mass spectrometry analyses (Fig. 4B–D).

Specifically, masses corresponding to faCOS of $(GlcNAc)_{1-9}$ units and the paCOS GlcN-$(GlcNAc)_{1-3,5-7}$, $(GlcN)_2$-$(GlcNAc)_{1-3}$, $(GlcN)_3$-$(GlcNAc)_{2,4}$, $(GlcN)_4$-$(GlcNAc)_5$ were detected (Fig. 4 and Table S1†). As expected, masses corresponding to $(GlcNAc)_2$ followed by $(GlcNAc)_3$ being the majority. Concerning paCOS, masses corresponding to GlcN-$(GlcNAc)_2$ followed of GlcN-$(GlcNAc)_3$ were the majority detected when using MNPs (Table S1†) but that of GlcN-GlcNAc followed by GlcN-$(GlcNAc)_2$ when using CMS (Table S2†). Pattern of products obtained could have been slightly altered due to the support used, which could alter the structure/specificity of the protein. Especially, considering that when free Chit42 was previously used in the hydrolysis of colloidal chitin only masses corresponding to the faCOS of $(GlcNAc)_{1-4}$ units and the paCOS GlcN-$(GlcNAc)_{2,4}$ and $(GlcN)_2$-$(GlcNAc)_3$ were detected. However, despite the high number of compounds detected in mass spectrometric analyses, only the faCOS of $(GlcNAc)_{1-3}$ units could be clearly identified due to the availability of the corresponding commercial standards. The data points to that immobilized Chit42 shows a higher range of product variability from colloidal chitin than the free enzyme. The possibility that immobilization could affect the adsorption of substrates in the enzyme active site modifying enzymatic activity, selectivity or even the final product profile was previously suggested.[31,33] Thus this was observed with glycosidases, such as the β-galactosidase from *Aspergillus oryzae*, and lipases from *Rhizopus oryzae* and *Candida antarctica*, which improved

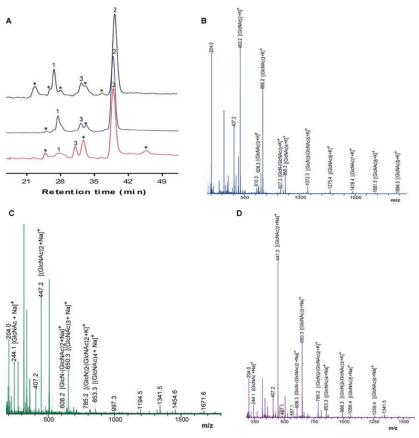

Fig. 4 Analysis of COS obtained from colloidal chitin. (A) High-performance anion exchange chromatography (HPAEC-PAD) analyses. The 24 h reactions catalyzed by immobilized Chit42 on MNPs (red) and CMS using GA linker (blue) and Gpn (black). Peaks: (1) GlcNAc; (2) $(GlcNAc)_2$; (3) $(GlcNAc)_3$; (*) Unidentified. MALDI-TOF MS analysis of the COS mixtures formed with the enzyme immobilized on (B) MNPs-GA, (C) CMS-GA and (D) CMS-Gpn. Data obtained with free Chit42 were previously indicated.[8] The peaks in the spectra correspond to the monoisotopic masses of hydrogen adducts $[M + H]^+$, $[M + K]^+$ and $[Ma + Na]^+$ of the COS. Only the major identified products were marked.

its selectivity and specificity after immobilization.[34–37] Structure of Chit42 was previously determined, and showed the expected folding described for chitinases included in the GH18 family with a characteristic groove shaped substrate-binding size able to accommodate at least six sugars units.[8] The unusual substrate-assisted catalytic mechanism of chitinases-GH18 requires a glutamic residue in the protein chain providing the acid protonating the glycosidic bond to be hydrolyzed and a mandatory GlcNAc residue in the substrate (after which to cut), which provides the oxygen (of the *N*-acetyl group) acting as nucleophile. Therefore, to the greater substrate acetylation degree, in principle, correspond both the greater hydrolysis and the diversity of products formed as previous reported.[8,37] This, together with the non-availability of commercial paCOS that could be used in the identification of products, led us to use the smallest available substrate with the highest degree of acetylation (chitosan QS2) in this section (Fig. 5). To our knowledge no paCOS produced by immobilized chitinases have been previously reported. It is conceivable that the use of supported enzymes (1 h contact time with substrate in a thermal shaker before products analysis) reduces substrate crystallinity making the crystalline regions more accessible to the hydrolytic enzyme activity, which would increase yield of low molecular weight products (see Table 2). This represents an interesting achievement for the industrial bioconversion of chitinolytic polymers, as with the use of supported enzymes the pretreatment of substrate could be avoided. Furthermore, Gpn is a better promising linker for immobilized chitinase in terms of enzymatic activity recover. This might be due to a greater mobility of the covalent bonded enzyme. Concerning the COS properties, and although there is no broad consensus on the results previously obtained, the size, degree and pattern of acetylation exert a notable influence on the physicochemical and biological activity of these molecules.[22,38–42] Thus, in general the lower MW COS the higher water solubility and lower viscosity, but also the lower antimicrobial activity and the higher antioxidant properties.[22,38] In addition, paCOS are excellent plant elicitors[39] and exhibit better antibacterial activity toward *Escherichia coli* and *Listeria monocytogenes* than COS fully acetylated.[43] This increases the biotechnological interest of the immobilized catalysts obtained in this work. However a deeper understanding on how the immobilized enzyme produces paCOS and the structural aspects involved in this process, as well as the development of improved methods for separation, characterization and quantification of products, will be essential to improve the enzyme activity/specificity to produce COS with different characteristics and, *a priori*, properties.

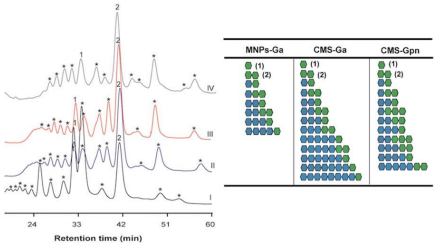

Fig. 5 HPAEC-PAD analysis of COS produced by the immobilized Chit42 with chitosan QS2 as substrate. On the right, a schematic representation of the polymerization degree and composition of reaction products predicted from mass spectrometry data (Tables S3 and S4†) is presented. Blue circles: GlcN. Green circles: GlcNAc. Identified peaks: (1) GlcNAc; (2) $(GlcNAc)_2$. Chromatograms obtained with (I) free enzyme; (II) MNPs-GA-Chit42; (III) CMS-GA-Chit42; (IV) CMS-Gpn-Chit42.

Conclusions

Chitinase Chit42 was successfully immobilized on magnetic nanoparticles and chitosan beads using GA and Gpn as intermediate linker, with a recovery of activity above 60%. The immobilized enzyme presented higher activity in acidic conditions and improved thermal resistance than free enzyme. Generated biocatalysts could be reused and have potential application in environmentally friendly production of fully acetylated and partially acetylated COS from colloidal chitin and chitosan wastes. The acidic and higher temperature operational stability of the immobilized chitinase Chit42 could be useful for the potential industrial application of this biocatalyst. The results show that the immobilized enzyme is more active than the free counterpart for COS production with widely variable size distribution depending on the type of chitosan used. These results envisage the use of immobilized chitinase for more efficient production of low molecular chitosan oligomers for biotechnological applications.

Experimental

Materials

Iron(III) chloride hexahydrated ($FeCl_3 \cdot 6H_2O$), ammonium iron(II) sulfate hexahydrate ($(NH_4)_2Fe(SO_4)_2 \cdot 6H_2O$), (3-aminopropyl)triethoxysilane (APTES), glutaraldehyde (GA; 25%) and sodium borohydride ($NaBH_4$) were from Sigma-Aldrich (St. Louis, America). Sodium hydroxide, ethanol and hydrochloric acid were from Merck (Germany). Genipin (Gpn), di-acetyl-glucosamine ($(GlcNAc)_2$), *N*,*N*′,*N*″-tri-acetyl-glucosamine ($(GlcNAc)_3$) were from Carbosynth Ltd (Berkshire, UK). Chitosan with different degree of deacetylation (DD) and polymerization (DP) were used, CHIT100 (100–300 kDa) and CHIT600 (600–800 kDa) all from shrimp shells (DD > 90%) were from Acros Organics (Geel, Belgium), chitosan QS1 from *Paralomis granulosa* (98 kDa, DD 81%) and chitosan QS2 from *Pandalus borealis* (31 kDa, DD 77%) from InFiQus (Madrid, Spain). Chitin (coarse flakes, DD ≤ 8%) from shrimp shells, chitosan CHIT50 (50–190 kDa, DD 77%), chitosan low molecular weight CHITLMW (50–190 kDa, DD ≥ 92%), *N*-acetyl-glucosamine and glucosamine (GlcN) were from Sigma-Aldrich (St. Louis, America).

Production of Chit42 in fed-batch fermenter

The chitinase Chit42 from *Trichoderma harzianum* CECT2413 fused to the *Saccharomyces cerevisiae* MFα1 secretion signal was previously cloned in plasmid pIB4 and expressed in *Pichia*

pastoris as referred.[8] The *P. pastoris* strain expressing chitinase Chit42 was cultivated to high cell density (for about 24 h) in 500 mL of BMG-F (13.4 mg mL^{-1} YNB, 4 mg mL^{-1} biotin, 1% (w/v) glycerol, 100 mM potassium phosphate, pH 6.0). Then this culture was grown in a 5 L bioreactor (Biostart BPluss Sartorius Ltd., Gottingen, Germany) containing 3.5 L of batch medium (40 g L^{-1} glycerol, 26.7 mL H_3PO_4 85%, 0.93 g L^{-1} $CaSO_4$, 18.2 g L^{-1} K_2SO_4, 14.9 g L^{-1} $MgSO_4$, 4.13 g L^{-1} KOH, 2 mL biotin (0.2 g L^{-1}), and 4.35 mL of PTM1 trace salts). The fermentation parameters were maintained at 30 °C, 600 rpm agitation, 20% dissolved oxygen and pH was controlled at 5.0 units with NH_4OH 28% (v/v) during 24 h (~40 OD_{600} units). Then 100% methanol was added continuously during 4 days at 20 μL min^{-1} L^{-1} of fermentation volume to induce the expression of protein Chit42 (final ~290 OD_{600} units). Culture growth was monitored spectrophotometrically at 600 nm (OD_{600}) and protein concentration using NanoDrop at 280 nm. To obtain the pure protein from the expression medium, the cells were removed by centrifuging at 6000 × *g* for 15 min, then the extracellular fraction was concentrated using 30 000 MWCO PES membranes in a Vivaflow 50 system (Sartorius, Gottingen, Germany).

Enzymatic activity analyses

Chitinase activity was evaluated by detection of reducing sugars produced from colloidal chitin and chitosan. Colloidal chitin preparation was obtained as previously reported.[8] For 1% (w/v) chitosan preparation, 1 g of solid materials was dissolved in 100 mL of 0.1 M acetic acid and then pH was adjusted to 5.0 with 1 M sodium acetate pH 5.5. For free enzyme, reactions were performed in 1.5 mL Eppendorf tubes by addition of 100 μL of the enzymatic solution (previously diluted in 70 mM potassium phosphate pH 5.5, if required) to 400 μL of 1% (w/v) colloidal chitin and other substrates. Tubes were incubated at 35 °C and 900 rpm in a Termo Shaker TS-100 (Boeco, Hamburg, Germany) during 1 h. Reactions were boiled for 10 min and one volume of 0.2 M NaOH was added. Polysaccharides were removed by centrifugation at 12 000 × *g* for 5 min. The quantification of reducing sugars in the supernatant was carried out using 3,5-dinitrosalicylic acid (DNS) method adapted to a 96-well microplate scale as described before.[8] A calibration curve of D-glucosamine (0–3 mg mL^{-1}) was used. The unit of chitinase activity (U) was defined as that corresponding to the release of 1 μmol of reducing sugar per minute (μmol min^{-1}).

Synthesis of magnetic nanoparticles (MNPs) and chitosan beads

Magnetic nanoparticles were prepared by the co-precipitation method according to Yamaura with some modifications.[23] Briefly, using a reflux condenser reactor 0.24 M of ammonium iron(II) sulfate hexahydrate solution was added to 0.25 M of iron(III) chloride hexahydrate solution at 60 °C under nitrogen gas (N_2) to suppress oxygen to avoid the iron(II) to undergo oxidation.[23] Then 1 M sodium hydroxide was added to obtain a final concentration of 0.5 M and the reaction was left for 1 h at room temperature. Particles were magnetically separated from the soluble phase and washed with distilled water until pH 7.0 was reached. MNPs were functionalized with amino groups by coating them with APTES according the procedure reported in.[44] Briefly, 1 g of nanoparticles were dispersed in 332 mL of absolute ethanol. A black powder was obtained after drying and grinding this reaction product. Then, 8 mL of APTES and 34.6 mL of 1 M HCl 1 M was added under agitation that was maintained for 16 hours. Particles were sequentially washed with ethanol (twice), water (one time), and finally dried with nitrogen flux.

Chitosan macro-spheres (CMS) were prepared from 2% (w/v) chitosan CHITLMW in 0.2 M acetic acid maintained with agitation for 16 hours at room temperature. Using a Cole Parmer™ Masterflex™ Brushless Pump System (Thermo Fisher Scientific), drop wise of viscous solution was coagulated using 0.5 M NaOH and 13% ethanol solution. The formed chitosan beads were washed with an excess of water until neutral pH was reached. The beads obtained were golden yellow, the same physical aspects as the ones already obtained in previous works.[32,45] When chitosan beads reacted with GA or Gpn their color changed to warm yellow or greenish blue, respectively, because the –C═N– imine bonds act as chromophore as reported when using GA.[46]

Characterization of magnetic nanoparticles and chitosan beads

The size and morphology of magnetic nanoparticles before and after the protein immobilization were analyzed by transmission electron microscopy (TEM Seiko JEOL Japan). A few micrograms of nanoparticles were suspended in water and then were sonicated. Dry chitosan macrospheres were coated with gold under vacuum before observation using scanning electron microscopy (SEM) for imaging at 11.500 μA and 15 kV accelerating voltage, using Zeiss DSM-950 (Zeiss, Oberkochen, Germany). The working magnification range was ×20–80 and higher magnification was not possible due to the bead's preparation instability.

Immobilization of Chit42

To immobilize the protein Chit42 to the generated MNPs and CMS particles, 0.05 g of nanoparticles and 0.2 g of wet chitosan beads, in separate Eppendorf tubes were used. Then 1 mL of 0.5% (v/v) GA in 100 mM potassium phosphate pH 7.0 was added. Tubes were incubated at 25 °C with agitation for 2 h. Particles were washed with the phosphate buffer to remove the excess of GA and then different concentrations of the protein Chit42 in the range of 3.12–24.8 mg g^{-1} of MNP or 0.78–6.2 mg g^{-1} of CMS were added. Tubes were maintained at 25 °C for 16 h with agitation. The MNPs-GA-Chit42 and CMS-GA-Chit42 immobilized catalysts were washed with 1 mL potassium phosphate two times to remove the unbound protein. Similar protocols were used to obtain the CMS-Gpn-Chit42 biocatalyst with Gpn (0.5% (w/v)) and CMS but using protein concentrations in the range 0.5–2.5 mg g^{-1}. Furthermore, the use of Gpn as linker for CMS ensures to have a fully non-toxic system for food grade applications of chitinases. The amount of the enzyme in the solutions before and after the immobilization process were measured by NanoDrop at 280 nm. The immobilization yield and activity recovery, both in percentage, were calculated as follows: immobilization yield (%) = 100 ×

(amount of protein immobilized/starting amount of protein) and the activity recovered yield (%) = 100 × (U_i/(U_a − U_w)). Where, amount of protein immobilized = amount of protein added for its immobilization − total amount of protein in washing buffer. U_i = activity (units) of Chit42 immobilized, U_a = activity (units) of Chit42 added and U_w = activity (units) of Chit42 in washing buffer. Different amounts of GA (0.5, 1 and 2% of GA solution) and Gpn (0.063, 0.125, 0.25, 0.312 and 0.5%; w/v) were also used to evaluate the optimal conditions for immobilization. GA 0.5% and Gpn 0.125% were selected as optimal conditions. The reduction of the Schiff base was done as previously referred.[41,47] In briefly, after washing the immobilized catalysts, 1 mg mL^{-1} of $NaBH_4$ in potassium phosphate pH 7.0 was added. Catalysts were maintained for 30 minutes at 25 °C with gentle stirring and then were washed three times with the referred phosphate buffer.

Biochemical characterization and reuse assay for the immobilized Chit42

Optimal pH of free and immobilized Chit42 was analyzed using colloidal chitin 1% (w/v) at different pH values, using 70 mM of sodium citrate (pH 3.0–5.0) or potassium phosphate (pH 5.0–8.0). Samples were incubated at 35 °C and 900 rpm in a Thermo Shaker TS-100 (Boeco, Hamburg, Germany) for 1 h. For optimal temperature assays, reactions including 70 mM potassium phosphate pH 5.0 and 1% (w/v) colloidal chitin were incubated in the range of 35–70 °C. For MNPs, biocatalysts were separated from the reaction mixture by applying magnetic field, and for CMS using centrifugation at 12 000 × *g* for 5 min. Then all reaction mixtures were boiled for 10 min. In reuse assays, 30 mg of chitosan beads, already attached to Chit42, and 0.6 mL of 1% (w/v) colloidal chitin pH 5.0 were incubated as explained above. Biocatalysts were precipitated at 1000 rpm 5 min and then the supernatant (200 μL) was mixed with DNS. For MNPs, 50 mg of support were used and reactions were developed as before but stopped by applying magnetic field to separate the catalysts from the mixture. Reducing sugars were analyzed by spectrophotometry at 540 nm after treatment at 100 °C for 10 min. MNPs and CMS were washed with 100 mM potassium phosphate pH 7.0 between each one of the reuse cycles.

COS production, characterization and quantification by HPAEC-PAD and mass spectrometry

Analysis of the products obtained by the hydrolytic activity of Chit42 immobilized to MNPs or CMS was carried out using 1% substrate (colloidal chitin and chitosan), incubation at 35 °C and 900 rpm as referred in previous section. Aliquots of 0.3 mL of reactions were mixed with an equal volume of 0.2 M NaOH, and centrifuged as referred. The supernatant was analyzed by HPAEC-PAD as described before.[8] The chromatography equipment was a Dionex ICS3000 system (Dionex, Thermo Fisher Scientific Inc., Waltham, MA) consisting of an SP gradient pump, an electrochemical detector with a gold working electrode and Ag/AgCl as reference electrode, and an auto sampler (model AS-HV). An anion-exchange 4 × 250 mm Carbo-Pack PA-100 column (Dionex) connected to a 4 × 50 mm CarboPac PA-100 guard column was used at 30 °C. The initial mobile phase was 4 mM NaOH at 0.3 mL min^{-1} for 30 min. Then, column was washed for 20 min at 0.5 mL min^{-1} with a solution containing 100 mM sodium acetate and 100 mM NaOH and further equilibrated with 4 mM NaOH. Standards of fully acetylated COS with DP ranging from 1 to 4 were used for identification of the reaction products. The molecular weight of COS was assessed by MALDI-TOF mass spectrometry using a mass spectrometer with Ultraflex III TOF/TOF (Bruker, Billerica, MA, USA) and an NdYAG laser. Registers were taken in positive reflector mode within the mass interval 40–5000 Da, with external calibration and with 20 mg mL^{-1} 2,5-dihydroxybenzoic in acetonitrile (3 : 7) (v/v) as matrix. Samples were mixed with the matrix in a 4 : 1 proportion and 0.5 μL were analyzed.

Funding

This work was supported by the EU EMFF-Blue Economy-2018-FISH4FISH-863697 project, the Spanish Ministry of Economy and Competitiveness [BIO2016-76601-C3-1/-2], the Spanish Ministry of Science and Innovation PID2019-105838RB-C32/-31, Fundación Ramón Areces [XIX Call of Research Grants in Life and Material Sciences], and by an institutional grant from Fundación Ramón Areces to the Centro de Biología Molecular. CSGI (Consorzio per lo Sviluppo dei Sistemi a Grande Interfase), Florence, Italy and MIUR for the Dipartimento di Eccellenza 2018-2022 grant are gratefully acknowledged.

Abbreviations

COS	Chitooligosaccharides
paCOS	Partially acetylated COS
GlcN	D-Glucosamine
GlcNAc	*N*-Acetyl-D-glucosamine
GH	Glycoside hydrolase
DP	Degree of polymerization
DD	Degree of deacetylation
MNPs	Magnetic nanoparticles
CMS	Chitosan macro-spheres

Conflicts of interest

The authors declare no competing financial interest.

Acknowledgements

The authors thank Asunción Martín-Redondo and Fadia Cervantes for technical support and advice on the use of equipment.

Notes and references

1 M. M. Abo Elsoud and E. M. El Kady, *Bull. Natl. Res. Cent.*, 2019, **43**, 59–70.
2 M. Rinaudo, *Prog. Polym. Sci.*, 2006, **31**, 603–632.

3 J. Zhou, X. Liu, F. Yuan, B. Deng and X. Yu, *ACS Sustainable Chem. Eng.*, 2020, **8**, 4781–4791.
4 M. Jiang, Z. Guo, C. Wang, Y. Yang, X. Liang and F. Ding, *Neurosci. Lett.*, 2014, **581**, 32–36.
5 P. Santos-Moriano, P. Kidibule, N. Míguez, L. Fernández-Arrojo, A. O. Ballesteros, M. Fernández-Lobato and F. J. Plou, *Catalysts*, 2019, **9**, 405–416.
6 M. B. Kaczmarek, K. Struszczyk-Swita, X. Li, M. Szczęsna-Antczak and M. Daroch, *Front. Bioeng. Biotechnol.*, 2019, **7**, 243–268.
7 P. Santos-Moriano, P. E. Kidibule, E. Alleyne, A. O. Ballesteros, A. Heras, M. Fernandez-Lobato and F. J. Plou, *Process Biochem.*, 2018, **73**, 102–108.
8 P. E. Kidibule, P. Santos-Moriano, E. Jiménez-Ortega, M. Ramírez-Escudero, M. C. Limón, M. Remacha, F. J. Plou, J. Sanz-Aparicio and M. Fernández-Lobato, *Microb. Cell Fact.*, 2018, **17**, 1–13.
9 I. A. Hoell, G. Vaaje-Kolstad and V. G. H. Eijsink, *Biotechnol. Genet. Eng. Rev.*, 2010, **27**, 331–366.
10 A. Oyeleye and Y. M. Normi, *Biosci. Rep.*, 2018, **38**, 1–21.
11 P. Torres-Salas, A. Del Monte-Martinez, B. Cutiño-Avila, B. Rodriguez-Colinas, M. Alcalde, A. O. Ballesteros and F. J. Plou, *Adv. Mater.*, 2011, **23**, 5275–5282.
12 R. A. Sheldon and S. van Pelt, *Chem. Soc. Rev.*, 2013, **42**, 6223–6235.
13 K. Wlizło, J. Polak, J. Kapral-Piotrowska, M. Graz, R. Paduch and A. Jarosz-Wilkołazka, *Catalysts*, 2020, **10**, 1–21.
14 M. Bilal, Y. Zhao, T. Rasheed and H. M. N. Iqbal, *Int. J. Biol. Macromol.*, 2018, **120**, 2530–2544.
15 W. Wang, N. Guo, W. Huang, Z. Zhang and X. Mao, *Catalysts*, 2018, **8**, 1–10.
16 S. Rouhani, A. Rostami and A. Salimi, *RSC Adv.*, 2016, **6**, 26709–26718.
17 T. J. Raharjo, L. Febrina, F. A. Wardoyo and R. T. Swasono, *Asian J. Biochem.*, 2016, **11**, 127–134.
18 C. A. Gasser, E. M. Ammann, A. Schäffer, P. Shahgaldian and P. F. X. Corvini, *Appl. Microbiol. Biotechnol.*, 2016, **100**, 7281–7296.
19 D. J. Seo, Y. H. Jang, R. D. Park and W. J. Jung, *Carbohydr. Polym.*, 2012, **88**, 391–394.
20 M. Prasad and P. Palanivelu, *Biotechnol. Appl. Biochem.*, 2015, **62**, 523–529.
21 S. Rathan and T. Thayumanavan, *J. Glob. Biosci.*, 2017, **6**, 5032–5045.
22 F. Liaqat and R. Eltem, *Carbohydr. Polym.*, 2018, **184**, 243–259.
23 M. Yamaura, R. L. Camilo, L. C. Sampaio, M. A. Macêdo, M. Nakamura and H. E. Toma, *J. Magn. Magn. Mater.*, 2004, **279**, 210–217.
24 F. Assa, H. Jafarizadeh-Malmiri, H. Ajamein, N. Anarjan, H. Vaghari, Z. Sayyar and A. Berenjian, *Nano Res.*, 2016, **9**, 2203–2225.
25 N. Zhang, R. X. Yan and W. Q. Guan, *Adv. Mater. Res.*, 2014, **936**, 674–680.
26 T. Mizuki, M. Sawai, Y. Nagaoka, H. Morimoto and T. Maekawa, *PLoS One*, 2013, **8**, 6–9.
27 J. -P. Chen and K. -C. Chang, *J. Chem. Technol. Biotechnol.*, 1994, **60**, 133–140.
28 M. A. Esawy, A. A. Gamal, M. M. I. Helal, M. E. Hassan, N. M. Hassanein and A. M. Hashem, *Int. J. Biol. Macromol.*, 2016, **92**, 56–62.
29 P. Santos-Moriano, J. M. Woodley and F. J. Plou, *J. Mol. Catal. B: Enzym.*, 2016, **133**, 211–217.
30 I. Eş, J. D. G. Vieira and A. C. Amaral, *Appl. Microbiol. Biotechnol.*, 2015, **99**, 2065–2082.
31 R. C. Rodrigues, C. Ortiz, Á. Berenguer-Murcia, R. Torres and R. Fernández-Lafuente, *Chem. Soc. Rev.*, 2013, **42**, 6290–6307.
32 T. Charoenwongpaiboon, K. Wangpaiboon, R. Pichyangkura and M. H. Prousoontorn, *RSC Adv.*, 2018, **8**, 17008–17016.
33 J. Palomo, *Curr. Org. Synth.*, 2009, **6**, 1–14.
34 C. Guerrero, C. Aburto, S. Suárez, C. Vera and A. Illanes, *Biocatal. Agric. Biotechnol.*, 2018, **16**, 353–363.
35 M. Ashjari, M. Mohammadi and R. Badri, *J. Mol. Catal. B: Enzym.*, 2015, **115**, 128–134.
36 O. Barbosa, R. Torres, C. Ortiz and R. Fernandez-Lafuente, *Process Biochem.*, 2012, **47**, 1220–1227.
37 A. Sørbotten, S. J. Horn, V. G. H. Eijsink and K. M. Vårum, *FEBS J.*, 2005, **272**, 538–549.
38 T. Laokuldilok, T. Potivas, N. Kanha, S. Surawang, P. Seesuriyachan, S. Wangtueai, Y. Phimolsiripol and J. M. Regenstein, *Food Biosci.*, 2017, **18**, 28–33.
39 S. Basa, M. Nampally, T. Honorato, S. N. Das, A. R. Podile, N. E. El Gueddari and B. M. Moerschbacher, *J. Am. Chem. Soc.*, 2020, **142**, 1975–1986.
40 L. Phil, M. Naveed, I. S. Mohammad, L. Bo and D. Bin, *Biomed. Pharmacother.*, 2018, **102**, 438–451.
41 H. Wu, B. B. Aam, W. Wang, A. L. Norberg, M. Sørlie, V. G. H. Eijsink and Y. Du, *Carbohydr. Polym.*, 2012, **89**, 511–518.
42 M. Mengíbar, I. Mateos-Aparicio, B. Miralles and Á. Heras, *Carbohydr. Polym.*, 2013, **97**, 776–782.
43 Á. Sánchez, M. Mengíbar, G. Rivera-Rodríguez, B. Moerchbacher, N. Acosta and A. Heras, *Carbohydr. Polym.*, 2017, **157**, 251–257.
44 R. Barbucci, D. Pasqui, G. Giani, M. De Cagna, M. Fini, R. Giardino and A. Atrei, *Soft Matter*, 2011, **7**, 5558–5565.
45 E. Biró, A. S. Németh, C. Sisak, T. Feczkó and J. Gyenis, *J. Biochem. Biophys. Methods*, 2008, **70**, 1240–1246.
46 L. Poon, L. D. Wilson and J. V. Headley, *Carbohydr. Polym.*, 2014, **109**, 92–101.
47 A. H. Orrego, M. Romero-Fernández, M. D. C. Millán-Linares, M. D. M. Yust, J. M. Guisán and J. Rocha-Martin, *Catalysts*, 2018, **8**, 1–15.

Supporting Information

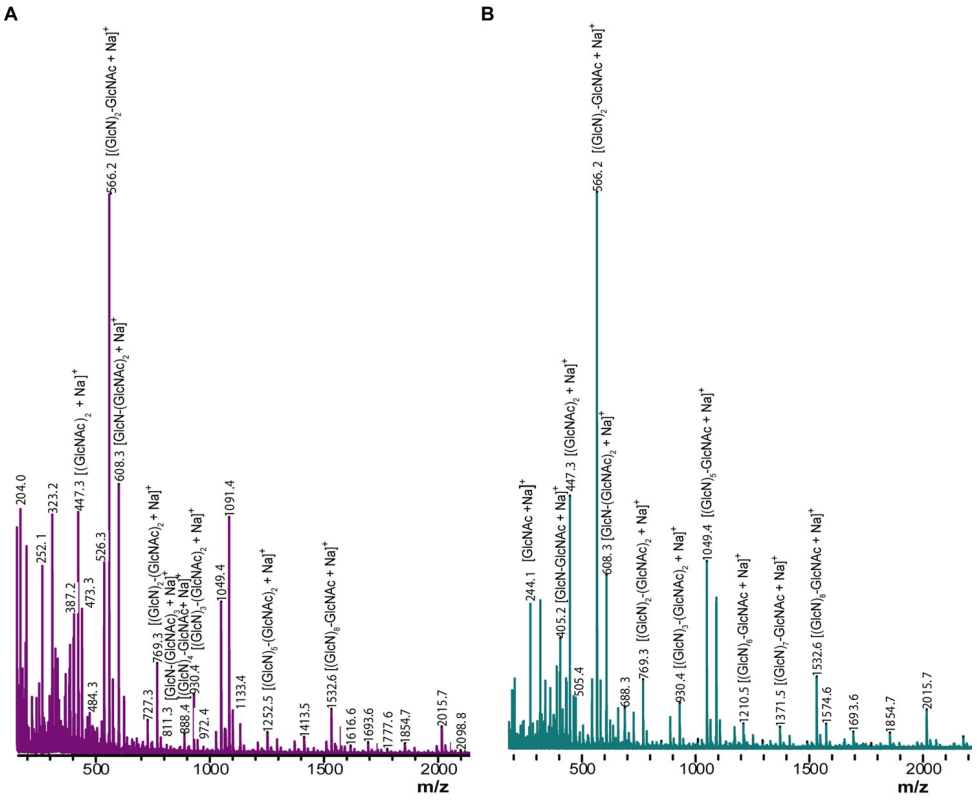

Fig. S1 MALDI-TOF MS analysis of COS produced from chitosan CHIT600

Table S1. Main peaks and intensities of the mass spectrum corresponding to the reaction mixture obtained with colloidal chitin as substrate and MNPs-Ga-Chit42.

m/z	Intensity (counts)	% intensity	Corresponding COS
204.048069	74792.8	97.1	Not identified
207.05111	2942.8	3.8	Not identified
222.069179	4040.5	5.2	$[GlcNAc + H]^+$
407.187317	35588.5	46.2	Not identified
410.105808	4425.5	5.7	Not identified
425.201267	9593.5	12.4	$[(GlcNAc)_2 + H]^+$
445.138071	3029.5	3.9	Not identified
447.172791	19739.5	25.6	$[(GlcNAc)_2 + Na]^+$
463.153265	77063.5	100.0	$[(GlcNAc)_2 + K]^+$
484.255273	1188	1.5	Not identified
487.126793	1814	2.4	Not identified
543.226817	571	0.7	Not identified
564.20866	702.5	0.9	Not identified
569.217362	721.5	0.9	Not identified
586.278685	909	1.2	$[GlcN-(GlcNAc)_2 + H]^+$
599.163938	547.3	0.7	Not identified
608.251569	597.5	0.8	$[GlcN-(GlcNAc)_2 + Na]^+$
610.270897	2974.5	3.9	Not identified
613.142247	868.5	1.1	Not identified
624.222527	2661.5	3.5	$[GlcN-(GlcNAc)_2 + K]^+$
625.176905	3654.5	4.7	Not identified
628.289805	3875.5	5.0	$[(GlcNAc)_3 + H]^+$
632.250583	605.5	0.8	Not identified
648.226479	2439.5	3.2	Not identified
650.258982	11187.5	14.5	$[(GlcNAc)_3 + Na]^+$
666.232806	55580.5	72.1	$[(GlcNAc)_3 + K]^+$
675.305591	599.5	0.8	Not identified
677.144182	527.5	0.7	Not identified
690.208849	994	1.3	Not identified
692.185592	564	0.7	Not identified
789.328882	568	0.7	$[GlcN-(GlcNAc)_3 + H]^+$
801.174723	314	0.4	Not identified
809.282388	296	0.4	Not identified
811.312296	460	0.6	$[GlcN-(GlcNAc)_3 + Na]^+$
817.156321	526	0.7	Not identified
827.282118	2589	3.4	$[GlcN-(GlcNAc)_3 + K]^+$
851.280029	640	0.8	Not identified
853.319461	2164	2.8	$[(GlcNAc)_4 + Na]^+$
869.295538	9576.5	12.4	$[(GlcNAc)_4 + K]^+$
885.28402	443.5	0.6	Not identified
911.291519	389.5	0.5	Not identified
989.296679	237.3	0.3	Not identified
1020.1958	178.3	0.2	Not identified

1030.33712	497.25	0.6	$[GlcN\text{-}(GlcNAc)_4 + K]^+$
1054.32442	239	0.3	Not identified
1056.36676	1059	1.4	$[(GlcNAc)_5 + Na]^+$
1072.34024	4313	5.6	$[(GlcNAc)_5 + K]^+$
1232.31246	430.5	0.6	Not identified
1233.35933	424.5	0.6	$[GlcN\text{-}(GlcNAc)_5 + K]^+$
1259.4089	519.5	0.7	$[(GlcNAc)_6 + Na]^+$
1274.32257	559.5	0.7	Not identified
1275.38132	2447.5	3.2	$[(GlcNAc)_6 + K]^+$
1436.43253	213.25	0.3	$[GlcN\text{-}(GlcNAc)_6 + K]^+$
1462.45593	411.25	0.5	$[(GlcNAc)_7 + Na]^+$
1478.42668	1456.25	1.9	$[(GlcNAc)_7 + K]^+$
1665.48702	157.5	0.2	$[(GlcNAc)_8 + Na]^+$
1681.47273	545	0.7	$[(GlcNAc)_8 + K]^+$
1884.54628	211.5	0.3	$[(GlcNAc)_9 + K]^+$

[M+H]+, [M+Na]+and [M+K]+peaks were detected in positive mode. Only main peaks in the refered mass interval was indicated.

Table S2. Main peaks and intensities of the mass spectrum corresponding to the reaction mixture obtained with colloidal chitin as substrate and CMS-Ga-Chit42 catalyst.

m/z	Intensity (counts)	% Intensity	Corresponding COS
204.049497	63304.0	64.2	Not identified
207.048784	6823.0	6.9	Not identified
222.072664	14991.8	15.2	$[GlcNAc + H]^+$
244.058167	44135.0	44.8	$[GlcNAc + Na]^+$
405.196503	5829.0	5.9	$[GlcN\text{-}GlcNAc + Na]^+$
407.193072	21113.0	21.4	Not identified
425.200914	5004.5	5.1	$[(GlcNAc)_2 + H]^+$
447.178884	98596.5	100.0	$[(GlcNAc)_2 + Na]^+$
463.169015	7959.5	8.1	$[(GlcNAc)_2 + K]^+$
567.138515	1876.0	1.9	Not identified
582.125896	2187.5	2.2	$[(GlcN)_2\text{-}GlcNAc + K]^+$
598.280917	1580.0	1.6	Not identified
608.247828	4381.0	4.4	$[GlcN\text{-}(GlcNAc)_2 + Na]^+$
628.292652	1968.0	2.0	$[(GlcNAc)_3 + H]^+$
650.259767	37585.0	38.1	$[(GlcNAc)_3 + Na]^+$
785.200548	3919.5	4.0	$[(GlcN)_2\text{-}(GlcNAc)_2 + K]^+$
811.321106	3218.0	3.3	$[GlcN\text{-}(GlcNAc)_3 + Na]^+$
818.357688	3247.0	3.3	Not identified
853.329302	9267.0	9.4	$[(GlcNAc)_4 + Na]^+$
863.394904	1232.0	1.2	Not identified
926.43638	957.5	1.0	Not identified
930.418239	840.5	0.9	$[(GlcN)_3\text{-}(GlcNAc)_2 + Na]^+$
965.415153	1019.5	1.0	Not identified
978.405773	809.0	0.8	Not identified
988.250199	989.5	1.0	$[(GlcN)_2\text{-}(GlcNAc)_3 + K]^+$
997.29935	1822.0	1.8	Not identified
1056.37761	2413.0	2.4	$[(GlcNAc)_5 + Na]^+$
1080.43919	627.5	0.6	Not identified
1102.47868	629.5	0.6	Not identified
1103.47238	677.5	0.7	Not identified
1172.48338	1499.5	1.5	Not identified
1194.47439	3195.5	3.2	Not identified
1216.50914	479.5	0.5	Not identified
1259.43605	1747.3	1.8	$[(GlcNAc)_6 + Na]^+$
1308.5221	578.3	0.6	Not identified
1319.52684	3141.0	3.2	Not identified
1327.5064	650.0	0.7	Not identified
1341.51589	7222.0	7.3	Not identified
1357.48522	576.0	0.6	Not identified
1373.47513	388.0	0.4	Not identified
1381.43992	358.0	0.4	Not identified
1396.7048	1652.3	1.7	Not identified
1418.68813	895.3	0.9	Not identified
1432.58457	2125.3	2.2	Not identified

1454.57385	3835.0	3.9	Not identified
1462.45176	925.0	0.9	$[(GlcNAc)_7 + Na]^+$
1470.56156	264.0	0.3	Not identified
1476.55369	358.0	0.4	Not identified
1486.51041	325.0	0.3	Not identified
1502.5326	498.0	0.5	Not identified
1524.53157	777.5	0.8	Not identified
1534.56763	363.5	0.4	Not identified
1546.60698	461.5	0.5	Not identified
1556.57897	449.5	0.5	Not identified
1568.59269	822.5	0.8	Not identified
1578.61127	692.5	0.7	Not identified
1607.59654	385.5	0.4	Not identified
1639.62893	368.0	0.4	Not identified
1649.59438	1079.0	1.1	Not identified
1665.51656	573.0	0.6	$[(GlcNAc)_8 + Na]^+$
1671.57778	2464.0	2.5	Not identified
1693.59516	384.0	0.4	Not identified
1733.62895	474.0	0.5	Not identified
1754.64212	1460.0	1.5	Not identified
1762.63655	473.0	0.5	Not identified
1778.77784	271.0	0.3	Not identified
1779.63603	301.0	0.3	Not identified
1784.67223	529.0	0.5	Not identified
1867.71615	248.5	0.3	Not identified
1970.73674	374.0	0.4	Not identified
1992.71992	340.0	0.3	Not identified
2008.70343	232.0	0.2	Not identified
2063.75732	239.0	0.2	Not identified
2191.84781	216.0	0.2	Not identified
2213.82604	234.0	0.2	Not identified

[M+H]+, [M+Na]+ and [M+K]+ peaks were detected in positive mode. Only main peaks in the referred mass interval was indicated.

Table S3. Main peaks and intensities of the mass spectrum corresponding to the reaction mixture obtained with chitosan QS2 as substrate and MNPs-Ga-Chit42

m/z	Intensity (counts)	% Intensity	Corresponding COS
244.075319	3733	15.4	$[GlcNAc + Na]^+$
375.223997	2945	12.2	Not identified
389.278401	5913	24.4	Not identified
405.185555	4582	18.9	$[GlcN\text{-}GlcNAc + Na]^+$
413.31406	1381	5.7	Not identified
415.258987	2513	10.4	Not identified
433.27943	8460	35.0	Not identified
447.209059	4097	16.9	$[(GlcNAc)_3 + Na]^+$
447.327028	24190	100.0	$[(GlcNAc)_2 + Na]^+$
463.313956	2216.5	9.2	$[(GlcNAc)_2 + K]^+$
473.311897	7506	31.0	Not identified
489.325217	945	3.9	Not identified
491.330494	1755	7.3	Not identified
505.373076	2892	12.0	Not identified
566.275309	1883	7.8	$[(GlcN)_2\text{-}GlcNAc + Na]^+$
608.283127	7899	32.7	[GlcN-(GlcNAc)2 + Na]+
624.249757	496	2.1	$[GlcN\text{-}(GlcNAc)_2 + K]^+$
727.317266	285	1.2	Not identified
769.336022	651.5	2.7	$[(GlcN)_2\text{-}(GlcNAc)_2 + Na]^+$
784.281839	287.5	1.2	Not identified
785.245001	324.5	1.3	$[(GlcN)_2\text{-}(GlcNAc)_2 + K]^+$
829.352002	276	1.1	Not identified
888.394671	200.5	0.8	$[(GlcN)_4\text{-}GlcNAc+ Na]^+$
904.261944	243.5	1.0	Not identified
930.370396	185	0.8	$[(GlcN)_3\text{-}(GlcNAc)_2 + Na]^+$
937.179722	221	0.9	Not identified
946.27019	504	2.1	$[(GlcN)_3\text{-}(GlcNAc)_2 + K]^+$
1091.44316	276.5	1.1	Not identified

[M+Na]+and [M+K]+peaks were detected in positive mode. Only main peaks in the referred mass interval was indicated.

Table S4. Main peaks and intensities of the mass spectrum corresponding to the reaction mixture obtained with chitosan QS2 as substrate and CMS-Ga-Chit42.

m/z	Intensity (counts)	% Intensity	Corresponding COS
244.080374	7309.5	25.7	$[GlcNAc + Na]^+$
375.23495	3029	10.6	Not identified
389.285895	7060	24.8	Not identified
405.197915	11661	40.9	$[GlcN\text{-}GlcNAc + Na]^+$
413.316033	1073	3.8	Not identified
415.275152	3150	11.1	Not identified
431.276659	953	3.3	Not identified
433.285972	8515	29.9	Not identified
447.21611	5845	20.5	$[(GlcNAc)_2 + Na]^+$
447.336815	28485	100.0	$[(GlcNAc)_2 + Na]^+$
453.363094	901	3.2	Not identified
459.306122	684	2.4	Not identified
463.316791	2804	9.8	$[(GlcNAc)_2 + K]^+$
473.319194	6373	22.4	Not identified
475.355835	10505	36.9	Not identified
489.310983	867.75	3.0	Not identified
491.339225	1512.75	5.3	Not identified
505.385862	2905.5	10.2	Not identified
544.29083	441	1.5	$[(GlcN)_2\text{-}GlcNAc + H]^+$
566.280329	10214	35.9	$[(GlcN)_2\text{-}GlcNAc + Na]^+$
575.226148	578	2.0	Not identified
582.258643	568	2.0	$[(GlcN)_2\text{-}GlcNAc + K]^+$
608.288274	12139.5	42.6	$[GlcN\text{-}(GlcNAc)_2 + Na]^+$
624.272157	773.5	2.7	$[GlcN\text{-}(GlcNAc)_2 + K]^+$
701.528964	2549	8.9	Not identified
727.344102	1287.5	4.5	$[(GlcN)_3\text{-}GlcNAc + Na]^+$
769.344413	2032	7.1	$[(GlcN)_2\text{-}(GlcNAc)_2 + Na]^+$
784.264092	413	1.4	Not identified
829.344771	303	1.1	Not identified
888.379382	620	2.2	$[(GlcN)_4\text{-}GlcNAc + Na]^+$
904.261931	351	1.2	$[(GlcN)_4\text{-}GlcNAc + K]^+$
930.387986	281	1.0	$[(GlcN)_3\text{-}(GlcNAc)_2 + Na]^+$
937.199359	515.75	1.8	Not identified
946.280822	413.75	1.5	$[(GlcN)_3\text{-}(GlcNAc)_2 + K]^+$
1049.43242	1089	3.8	$[(GlcN)_5\text{-}GlcNAc + Na]^+$
1091.43683	276	1.0	Not identified
1210.4502	267.5	0.9	$[(GlcN)_6\text{-}GlcNAc + Na]^+$
1252.49444	139	0.5	Not identified
1371.51045	193	0.7	$[(GlcN)_7\text{-}GlcNAc + Na]^+$
1532.54891	166.5	0.6	$[(GlcN)_8\text{-}GlcNAc + Na]^+$

$[M+H]^+$, $[M+Na]^+$ and $[M+K]^+$ peaks were detected in positive mode. Only main peaks in the referred mass interval was indicated.